Chapter 3

Stratigraphic and Petrological Insights into the Late Jurassic–Early Cretaceous Tectonic Framework of the Northwest Pacific Margin

Reishi Takashima, Hiroshi Nishi and
Takeyoshi Yoshida

Additional information is available at the end of the chapter

http://dx.doi.org/10.5772/intechopen.68289

Abstract

Late Jurassic–Early Cretaceous volcano-sedimentary sequences in the Sorachi, Kumaneshiri, and Yezo groups are exposed in central Hokkaido. The sequences are considered to reflect the Late Mesozoic tectonic history of the northwest Pacific continental margin. Based on the stratigraphic and petrological characteristics of igneous and volcaniclastic rocks of the Sorachi, Yezo, and Kabato groups, Late Jurassic–Early Cretaceous tectonics in central Hokkaido can be divided into six stages. Stage I (Tithonian) is characterized by extensive eruption of tholeiitic basalt accompanied with andesitic volcaniclastic rocks and terrigenous deposits. Seafloor spreading or large igneous province formation occurred near an island arc and/or continent during this stage. In Stage II, island arc volcanic islands were constructed on the basaltic rocks formed during Stage I. Stage III (latest Berriasian-Valanginian) is characterized by the formation of pull-apart basins accompanied by seafloor spreading. Widespread upwelling of the asthenosphere below central Hokkaido may have occurred during this stage. After the cessation of in situ volcanism in Stage IV (Hauterivian), submarine island arc volcanism reoccurred in Stage V (Barremian). In Stage VI (Aptian–Campanian), typical active continental margin volcanism occurred and voluminous granitic batholiths were formed in western Hokkaido.

Keywords: Jurassic, Cretaceous, Sorachi group, Kumaneshiri group, Asian continental margin, Hokkaido

1. Introduction

The Early Late Jurassic is characterized by a peak in submarine igneous activity represented by a negative peak in $^{87}Sr/^{86}Sr$ in marine sediments [7, 15]. The spreading rate of the mid-oceanic ridges increased in the Central Atlantic and Piemonte-Ligurian oceans [13, 37], when large igneous provinces (LIPs), such as the Shatsky Rise, formed in the Pacific. The active volcanism during this period was likely associated with significant global warming and transgression. Consequently, the Late Jurassic–Early Cretaceous was characterized by significant reconfiguration of the continents in East Asia. During this period, the Siberia Block (SB) collided with both the combined block of the Central Asian Orogenic Belt (CAOB)–North China Block (NCB)–South China Block (SCB) and the Omolon–Kolyma Block (OKB) along its southern and eastern margins, respectively [22, 36, 41]. These collisions resulted in the formation of the very large, amalgamated Asian continent and may have been reflected in the tendency for long-term increases in $^{87}Sr/^{86}Sr$ in marine sediments. The extensive upwelling of the asthenospheric mantle that occurred along the eastern Asian margin slightly after these collisions induced the renewal of the Asian continental crust, development of the NE–SW-trending extensional basins, and the extensive felsic volcanism referred to as the Late Yanshanian Event, which is considered to have started in the Late Jurassic and culminated in the late Early Cretaceous [14, 40].

The Japanese islands were part of the active continental margin of Asia until the opening of the Japan Sea in the Miocene. Of the Japanese islands, Hokkaido Island and the northeastern part of Honshu Island are considered to have been located on the supra-subduction magmatic zone–convergent boundary between the Paleo-Pacific Plate and the South China Block during the Early Cretaceous [27, 31]. The western part of Hokkaido Island is well suited for reconstructing the spatiotemporal characteristics of geodynamic evolution across the supra-subduction zone because the strata from the accretionary complex to the magmatic zones are intermittently well exposed. This paper examines the geodynamic processes of Late Jurassic–Early Cretaceous Hokkaido based on the sedimentary facies and geochemistry of volcaniclastic and igneous rocks.

2. Regional geologic setting

The Mesozoic rocks on western Hokkaido are divided into the N–S-trending tectonic divisions of the Oshima, Rebun–Kabato, and Sorachi–Yezo belts (**Figure 1**), which are considered to have formed along the west-dipping subduction zone of the Pacific oceanic plates under the eastern margin of the Asian continent [21].

The Oshima Belt consists mainly of a Jurassic accretionary complex and middle–Late Cretaceous granitic rocks (**Figure 2**). The Early Cretaceous volcano-sedimentary sequences, referred to as the Rebun and Kabato groups, are exposed along the eastern margin of the Oshima Belt. The distribution of the Rebun and Kabato groups is distinguished as the Rebun–Kabato Belt. The Sorachi–Yezo Belt is represented by a coherent succession consisting of the uppermost Jurassic ophiolite (Horokanai ophiolite), uppermost Jurassic–Lower Cretaceous submarine volcano-sedimentary sequences (Sorachi Group), and Lower Cretaceous–Paleogene submarine terrigenous sequences (Yezo Group), in ascending order (**Figure 2**). The early Cretaceous accretionary complexes are exposed in the central (Kamuikotan Zone) and eastern (Idonnappu Zone) parts of the Sorachi–Yezo Belt. Although both are accretionary

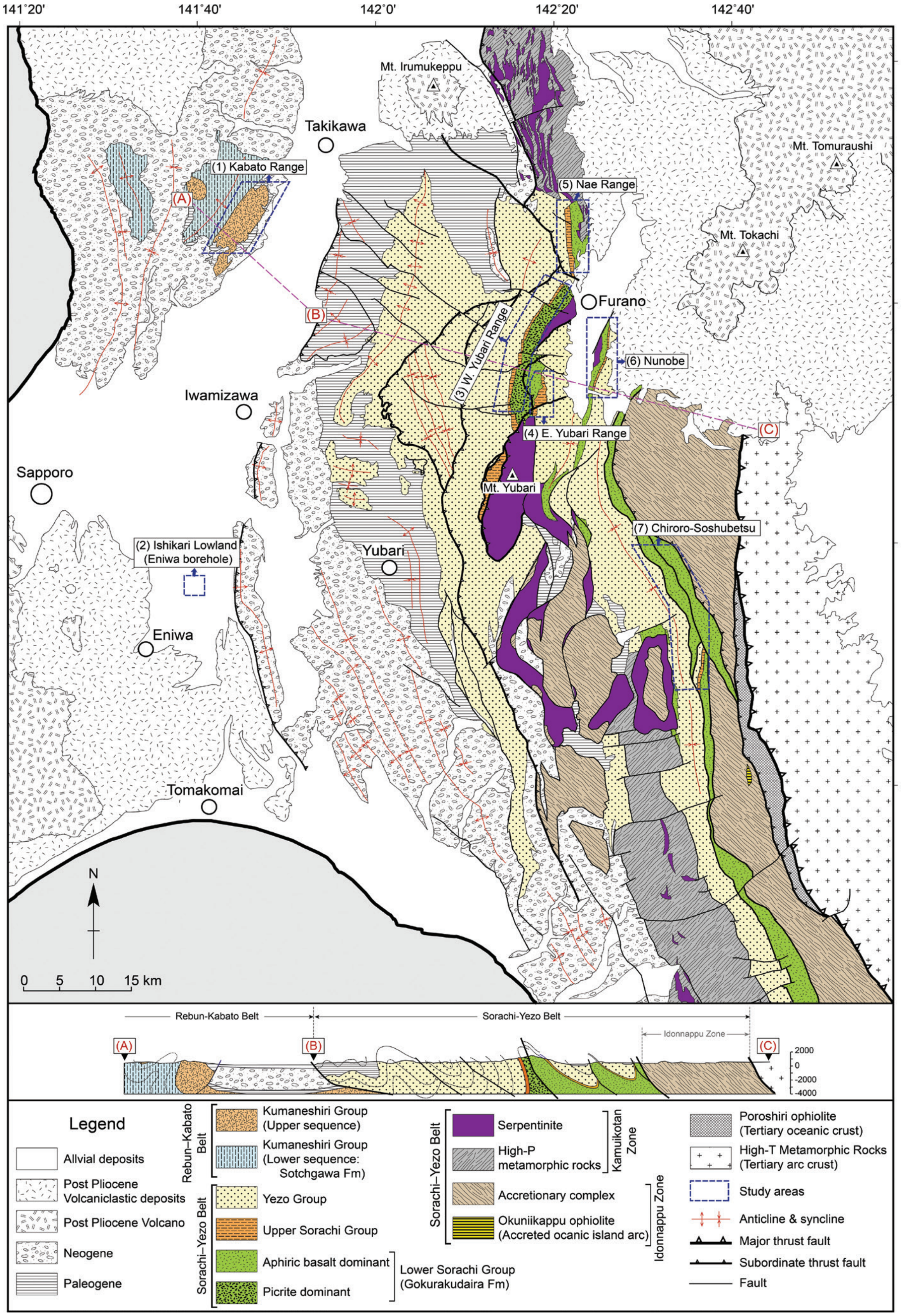

Figure 1. Geologic map and structural profile of central Hokkaido.

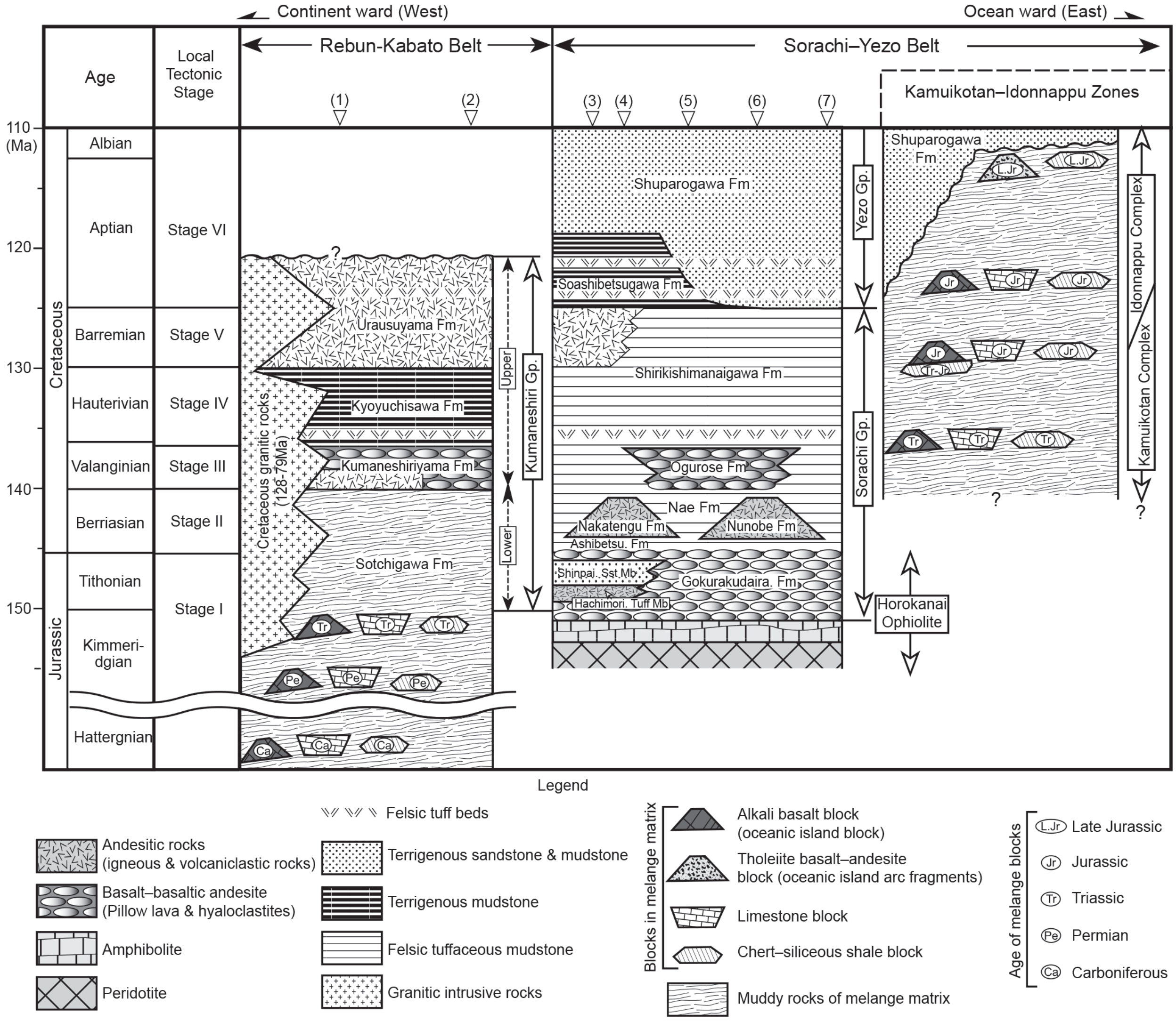

Figure 2. Schematic profile of Late Jurassic–Early Cretaceous arc-trench system in Hokkaido. Studied areas include (1) Kabato Range, (2) Ishikari Lowland (Eniwa borehole), (3) areas west of Yubari Range, (4) areas east of Yubari Range, (5) Nae Range, (6) Nunobe, and (7) Soshubetsu–Chiroro.

complexes showing a trend of becoming younger toward the east [11, 35], the former is high-pressure metamorphosed.

3. Stratigraphy of the upper Jurassic–Lower Cretaceous volcano-sedimentary succession in Hokkaido

Upper Jurassic–Lower Cretaceous volcano-sedimentary sequences of the Rebun–Kabato and Sorachi–Yezo belts occur in seven areas (**Figures 1**–**3**): (1) Kabato Range, (2) Ishikari Lowland (Eniwa borehole), (3) west of Yubari Range, (4) east of Yubari Range, (5) Nae Range, (6) Nunobe, and (7) Soshubetsu–Chiroro from west to east (**Figures 1** and **2**). The volcano-sedimentary sequences in the former two areas are named the Kumaneshiri Group, while the others are named the Sorachi and Yezo groups (**Figures 2** and **3**).

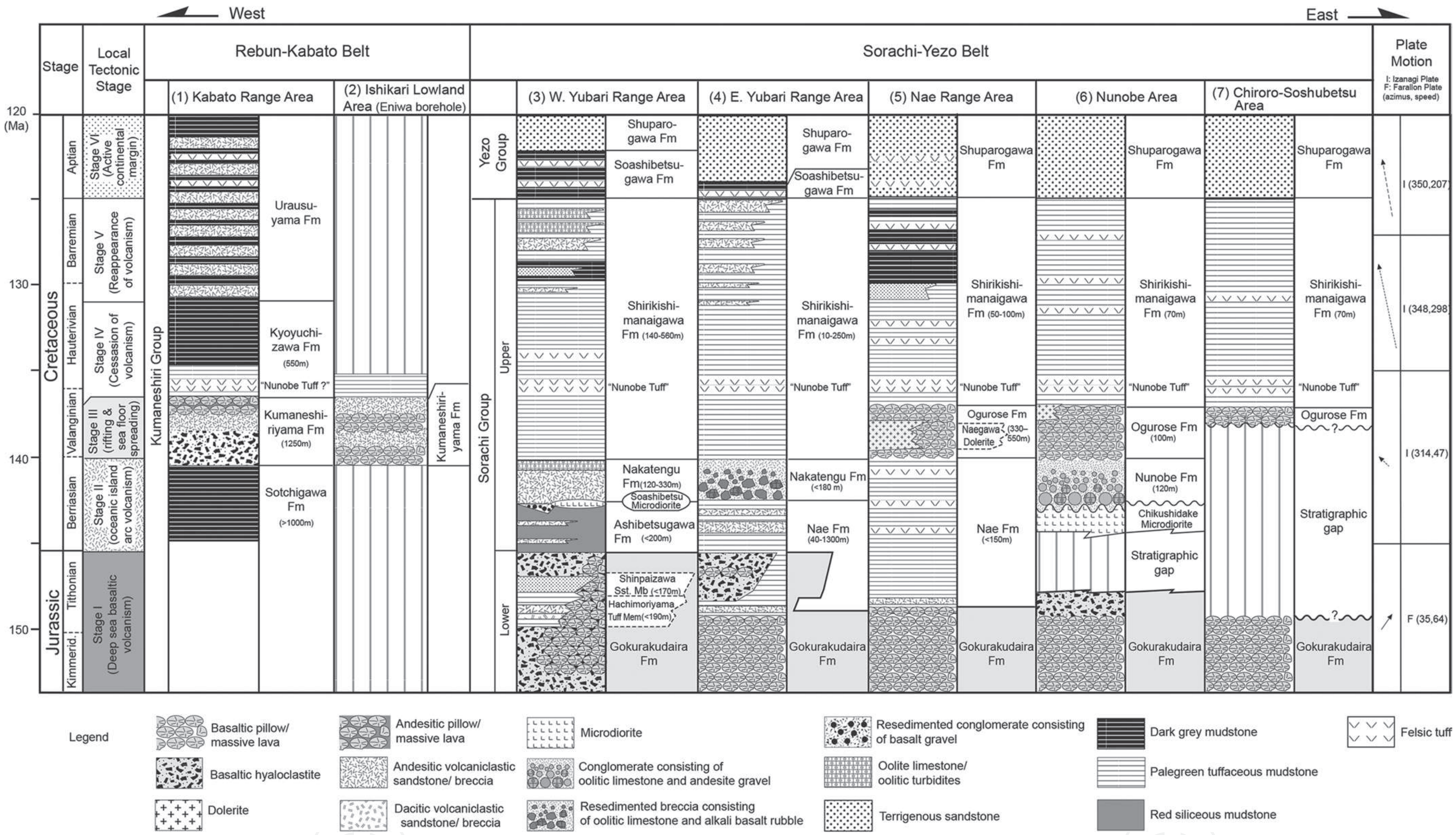

Figure 3. Generalized isochronous stratigraphic nomenclature of the Sorachi, Yezo, and Kumaneshiri groups in the seven studied sections (modified from Ref. [31]).

3.1. Kumaneshiri Group

The Kumaneshiri Group is represented by the Lower Cretaceous volcano-sedimentary sequences exposed in the Rebun–Kabato Belt, and consists mainly of submarine volcanic and sedimentary rocks (**Figure 3**). The group is made up of the Sotchigawa Formation, Kumaneshiriyama Formation, Kyoyuchizawa Formation, and Urausuyama Formation, in ascending order, and accompanied by basaltic-to-andesitic intrusive rocks.

The Sotchigawa Formation consists mainly of dark gray shale with occasional intercalations of sandstones and basaltic to rhyolitic tuff beds. Folding and faulting prevailed in these strata, which had a total thickness of approximately 2000 m. Radiolarian fossils assigning the Late Jurassic to Early Cretaceous period occur in this formation [12].

The Kumaneshiriyama Formation is mainly composed of volcaniclastic rocks with subordinate amounts of mudstone and pillow lava. The lava and rubble of the volcaniclastic rocks are olivine–clinopyroxene-phyric basalt and clinopyroxene–plagioclase-phyric basaltic andesite. Based on radiolarian biostratigraphy, the 500–1250 m-thick formation is correlative with the Late Berriasian to Valanginian [17, 26].

The Kyoyuchizawa Formation is a 600-m thick sequence consisting of dark gray and greenish gray mudstone with intercalations of rhyolitic fine-grained tuff beds. A 30-m sequence consisting of greenish gray mudstone frequently intercalated with rhyolitic tuff beds occurs at the basal part of this formation. This lithology resembles the "Nunobe Tuff Member" of the Sorachi Group described in Section 3.2.

The Urausuyama Formation is composed of alternating beds of basaltic-to-andesitic volcaniclastic sandstone and black mudstone. The thickness of this formation has been estimated to be approximately 1300–1600 m. Basaltic-to-andesitic volcanic breccia occurs intermittently in the upper part of this formation, and the rubble of volcanic breccia is composed of clinopyroxene–plagioclase-phyric basaltic andesite and clinopyroxene–plagioclase-phyric basaltic andesite. Radiolarian fossils obtained from the Kyoyuchizawa and Urausuyama formations imply that these formations are younger than Berriasian [17].

3.2. Sorachi Group

The Sorachi Group ranges from the Latest Jurassic to Barremian, and consists mainly of submarine volcanic and volcaniclastic rocks. Since the rocks of the Sorachi Group are laterally discontinuous [31], the Sorachi Group is divided into four rock assemblages based on the age and characteristics of the igneous rocks: (1) Uppermost Jurassic (tholeiitic basaltic rock assemblage), (2) Berriasian (andesitic rock assemblage), (3) Valanginian (basaltic rock assemblage), and (4) Hauterivian-Barremian (tuffaceous rock assemblage).

3.2.1. Uppermost Jurassic tholeiitic basaltic rock assemblage

The Gokurakudaira Formation and the lower part of the Nae Formation constitute this rock assemblage (Stage I rocks in **Figure 3**). The Gokurakudaira Formation is composed of basaltic pillow lava and hyaloclastite. Petrographic characteristics of the basalt in this formation differ among areas. For example, areas to the east of the Yubari Range, Nae Range, and Soshubetsu–Chiroro [areas (4), (5), and (7) in **Figures 1–3**] are composed of aphyric basalt, while those to the west of the Yubari Range [area (3) in **Figures 1–3**] are predominated by picrite. The basalt in the Nunobe area [area (6) in **Figures 1–3**] is mostly aphyric basalt, but the hyaloclastites in the uppermost part are olivine-phyric andesite. To the west of the Yubari Range, the Gokurakudaira Formation intercalates the Hachimoriyama Tuff Member and the Shinpaizawa Sandstone Member. The former member consists of tuffaceous mudstone and intercalates abundant dacitic-to-andesitic volcaniclastic rocks, while the latter is predominantly sandstone with alternating beds of terrigenous turbidite sandstone and hemipelagic mudstone. To the southeast of the Yubari Range, basaltic rocks intercalate thick tuffaceous mudstone that is correlated with the lower part of the Nae Formation. In this area, basalts below the tuffaceous mudstone consist mainly of pillow lava, while those above the tuffaceous mudstone are predominated by hyaloclastite.

The Nae Formation consists of pale green tuffaceous mudstone frequently intercalated with felsic tuff beds. However, the lower part of this formation rarely intercalates thin beds of andesitic volcaniclastic sandstone.

In terms of radiolarian biostratigraphy, the first occurrence of *Pseudodictyomitra carpatica*, which is assigned to be Tithonian, was identified at the lower part of the Hachimoriyama Tuff Member and the Nae Formation [31].

3.2.2. Berriasian andesitic rock assemblage

The Berriasian rock assemblage (Stage II rocks in **Figure 3**) of the Sorachi Group, which is constituted by the Ashibetsugawa, Nae, Nakatengu, and Nunobe formations, is accompanied with intrusive rocks of the Soashibetsu and Chikushidake microdiorites (**Figures 2** and **3**). Although [31] described the Soashibetsu and Chikushidake microdiorites as "micromonzonites," we have revised this here as the highly alkaline nature of these rocks may have resulted from secondary alteration.

To the west of the Yubari Range, the Ashibetsugawa Formation conformably overlies the basaltic hyaloclastite and/or pillow lava of the Gokurakudaira Formation. The Ashibetsugawa formation is composed mainly of red mudstone and frequently intercalates basaltic-to-andesitic volcaniclastic sandstone beds. The Nakatengu Formation, which covers conformably the Ashibetsugawa Formation, consists of andesitic volcaniclastic breccia. The basaltic conglomerate and oolitic turbidite beds occur at the base and top of this formation, respectively. The Soashibetsu microdiorite intrudes the border between the Ashibetsugawa and Nakatengu formations.

To the east of the Yubari and Nae ranges, the pale green tuffaceous mudstone of the Nae Formation conformably overlies the basaltic rocks of the Gokurakudaira Formation. Although the tuffaceous mudstone occurs throughout this interval in the Nae Range area, the Nakatengu Formation overlies the Nae Formation on the eastern side/to the east of the Yubari Range. The Nakatengu Formation on the east of the Yubari Range is composed of matrix-supported conglomerate beds containing sub-rounded rubble of alkali basalt and oolite limestones. Based on their sedimentological characteristics, the beds have been interpreted to be gravity flow deposits [31].

In the Nunobe area, Chikushidake microdiorite is unconformably covered by the basal conglomerate of the Nunobe Formation. The conglomerate is clast supported, and consists of subangular to sub-rounded rubble composed of andesite, oolite limestone, and microdiorite. The conglomerate grades into sandstone further upward [29].

3.2.3. Late Berriasian–Late Valanginian basaltic rock assemblage

Rocks of this interval are represented by the Ogurose Formation and the lower part of the Shirikishimanaigawa Formation (Stage III rocks of **Figure 3**). The Ogurose Formation occurs in the Nae Range and Nunobe areas, and consists of basaltic pillow lava and dolerite dikes. Pillow lobes are generally larger than those of the Gokurakudaira Formation and contain numerous bubbles. To the west and east of the Yubari Range, basaltic rocks are absent in the contemporaneous strata which consist mainly of pale green tuffaceous mudstone belonging to the lower part of the Shirikishimanaigawa Formation (**Figures 2** and **3**).

3.2.4. Late Valanginian–Barremian siliceous mudstone rock assemblage

The rocks of this interval are represented by the Shirikishimanaigawa Formation and are characterized by a predominance of pale green tuffaceous siliceous mudstone (Stage IV and V rocks of **Figure 3**). To the west of the Yubari Range, andesitic volcaniclastic sandstone beds and felsic tuff beds are intercalated in the upper part of the Shirikishimanaigawa Formation.

At an interval of several meters to several tens of meters, white siliceous felsic tuffs are intercalated frequently at the lower part of the Shirikishimanaigawa Formation. This interval is referred to here as the "Nunobe Tuff", and is traceable throughout the studied areas (**Figures 2** and **3**).

3.2.5. Post-Aptian rock assemblage

This rock assemblage is constituted by the Yezo Group, which ranges from the Aptian to the Paleocene [30] (Stage VI rocks of **Figure 3**). The Yezo Group consists mainly of hemipelagic mudstone and turbidite sandstone that were accumulated in a fore-arc basin along the active Asian continental margin. Since the Yezo Group yields abundant marine macro- and microfossils as well as felsic tuffs, numerous stratigraphic and paleoenvironmental studies have been carried out [1, 3, 8, 20, 24, 32–34].

The Yezo Group consists of the Soashibetsu, Shuparogawa, Maruyama, Hikagenosawa, Saku/Mikasa, Kashima/Haborogawa, and Hakobuchi formations, in ascending order [30]. The rhyolite fragments were taken from the volcaniclastic breccias which occur at the base of the Maruyama Formation. The Maruyama Formation is in the *Biticinella breggiensis* planktonic foraminiferal Zone, which ranges around 105–102 Ma [20, 24].

4. Geochemical analysis of igneous rocks

The igneous rocks and rubble of volcaniclastic rocks of the Kumaneshiri and Sorachi and Yezo groups were analyzed for major and trace elements. The samples from the Kumaneshiri Group

http://dx.doi.org/10.5772/intechopen.68289

in the Ishikari Lowland were obtained from the Eniwa SK-1 borehole, and were provided by Japan Petroleum Exploration Co., Ltd. (JAPEX).

Major and trace elements in the samples were identified using X-ray fluorescence spectrometry at the Faculty of Education, Fukushima University. FeO was analyzed by titration, and the H_2Ot contents were determined after ignition. Rare earth elements (REEs) were analyzed using an inductively coupled plasma mass spectrometer (ICP-MS) at the Geoanalytical Laboratory, Washington State University. Analytical results of the Gokurakudaira Formation were also obtained from Ref. [28]. All of the presented data are available from the Osaka Prefecture University Education and Research Archives (OPERA) (http://hdl.handle.net/10466/14732).

5. Results

Rocks of the Kumaneshiri and Sorachi groups consist of submarine volcanic and volcaniclastic rocks and mudstone; lithological correlation among areas was difficult because of lateral changes in lithology. Takashima et al. [31] correlated the sequences of the Sorachi Group with radiolarian data. Specifically, they examined the first occurrence of *P. carpatica* and the first and last occurrences of "*Cecrops*" *septemporatus*, and then divided the Sorachi Group into four stages based on lithologic features (Stages I–IV). Several horizons of the Kumaneshiri Group can also be correlated with these stages based on radiolarian biostratigraphy and the "Nunobe Tuff". Based on the lithological characteristics of the Kumanishiri Group, Stage IV of [31] can be subdivided into two stages because the interval of their stage IV includes the Kyoyuchizawa and Urausuyama formations in the Rebun–Kabato Belt. We redefine their Stage IV as being equivalent to the depositional interval of the Kyoyuchizawa Formation and the lower part of the Shirikishimanaigawa Formation (Late Valanginian–Hauterivian), and consider that Stage V can be correlated to the depositional interval of the Urausuyama Formation and the upper part of the Shirikishimanaigawa Formation (Barremian). Furthermore, we consider that Stage VI includes the deposition interval of the Yezo Group (Aptian–Paleocene).

Stratigraphic and areal changes in SiO_2–Nb/Y, a spider diagram of incompatible trace element abundance relative to N-MORB, and REE abundance relative to chondrite, are shown in **Figures 4–6**.

5.1. Rocks of Stage I (Kimmeridgian–Tithonian): Gokurakudaira Formation and the lower part of the Nae Formation

The basaltic rocks of the Gokurakudaira Formation consist mainly of tholeiitic basalts, which have a mid-ocean ridge basalt (MORB)-like flat pattern in N-MORB-normalized incompatible trace-element abundance (**Figures 4** and **5**). Conversely, the picrites and olivine-phyric andesites from the areas to the west of the Yubari Range and Nunobe are depleted in all elements, N-MORB-normalized incompatible trace elements, and REE abundances. Compared to heavy REEs (HREEs), the picrites and olivine-phyric andesites are also depleted in light REEs (LREEs) (**Figures 5** and **6**). Although basaltic rocks occur in two horizons to the east of the Yubari Range, their compositions are similar.

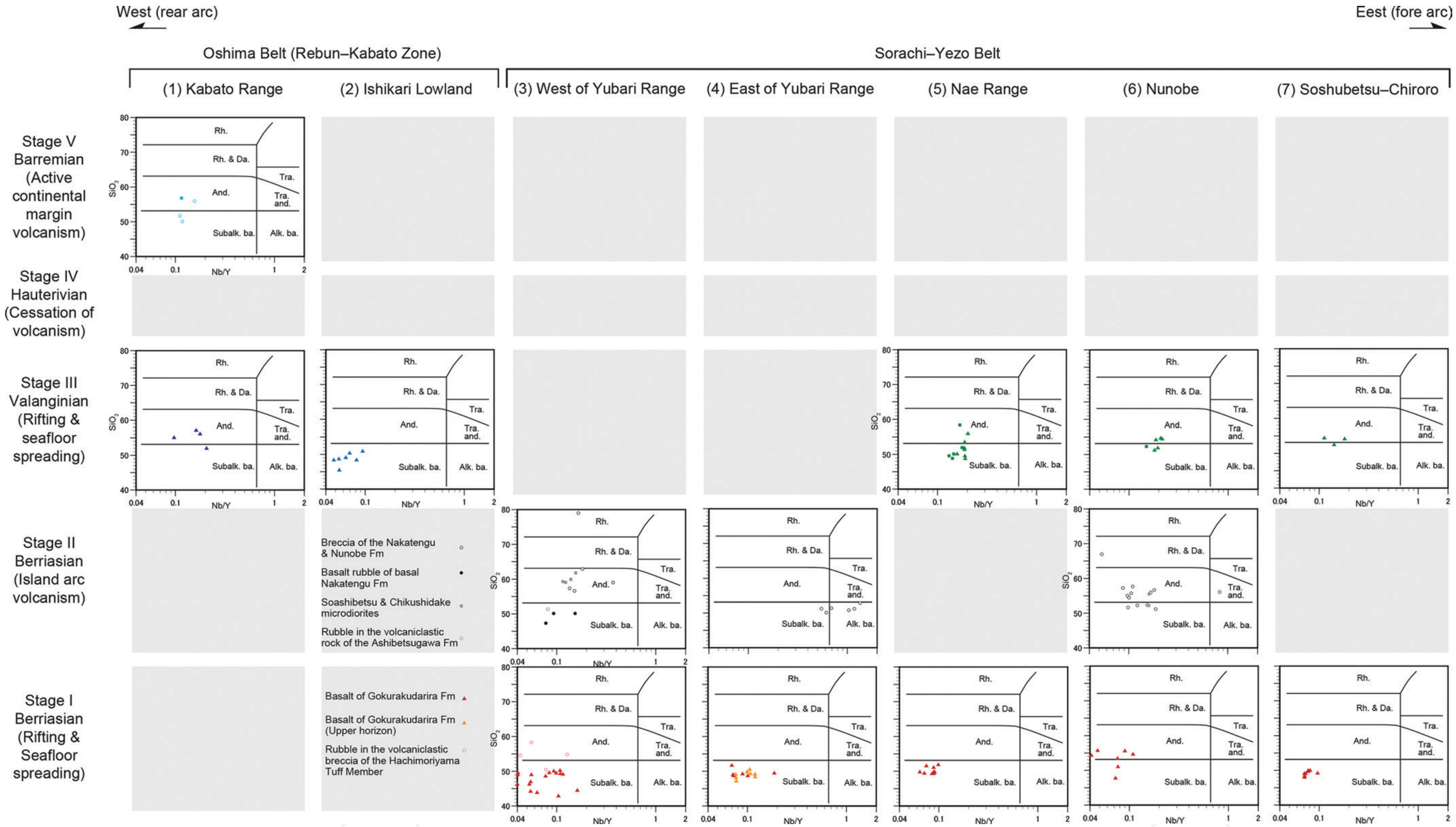

Figure 4. Plot of SiO_2 versus Nb/Y for igneous rocks from the Sorachi and Kumaneshiri groups in the studied sections. Fields are from Ref. [39]. Triangular, square, and circular symbols show extrusive rocks, intrusive rocks, and rubble in the volcaniclastic rocks, respectively.

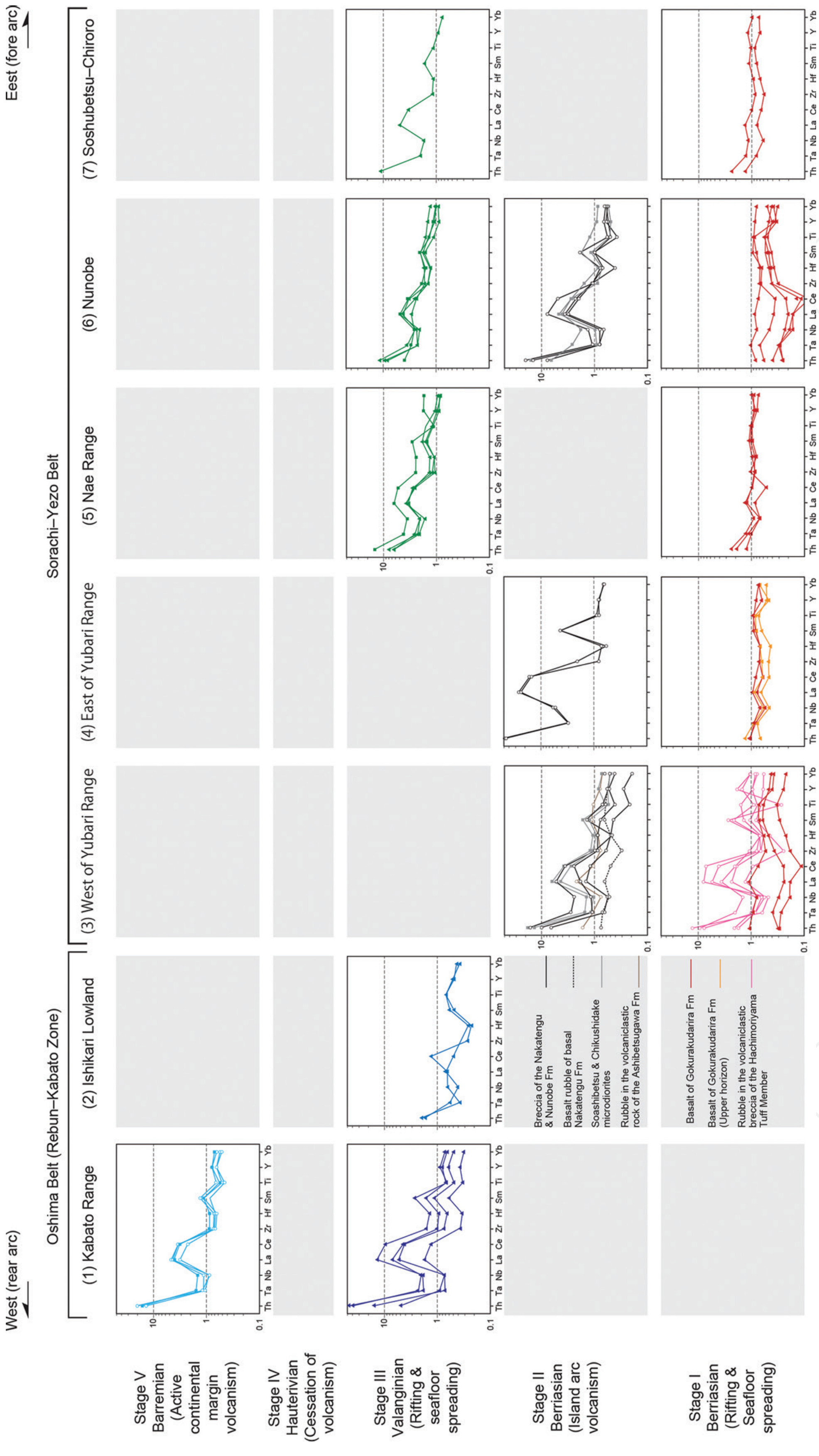

Figure 5. N-MORB-normalized incompatible trace element patterns [25] for igneous rocks from the Sorachi and Kumaneshiri groups in the studied sections. Symbols as in **Figure 4**.

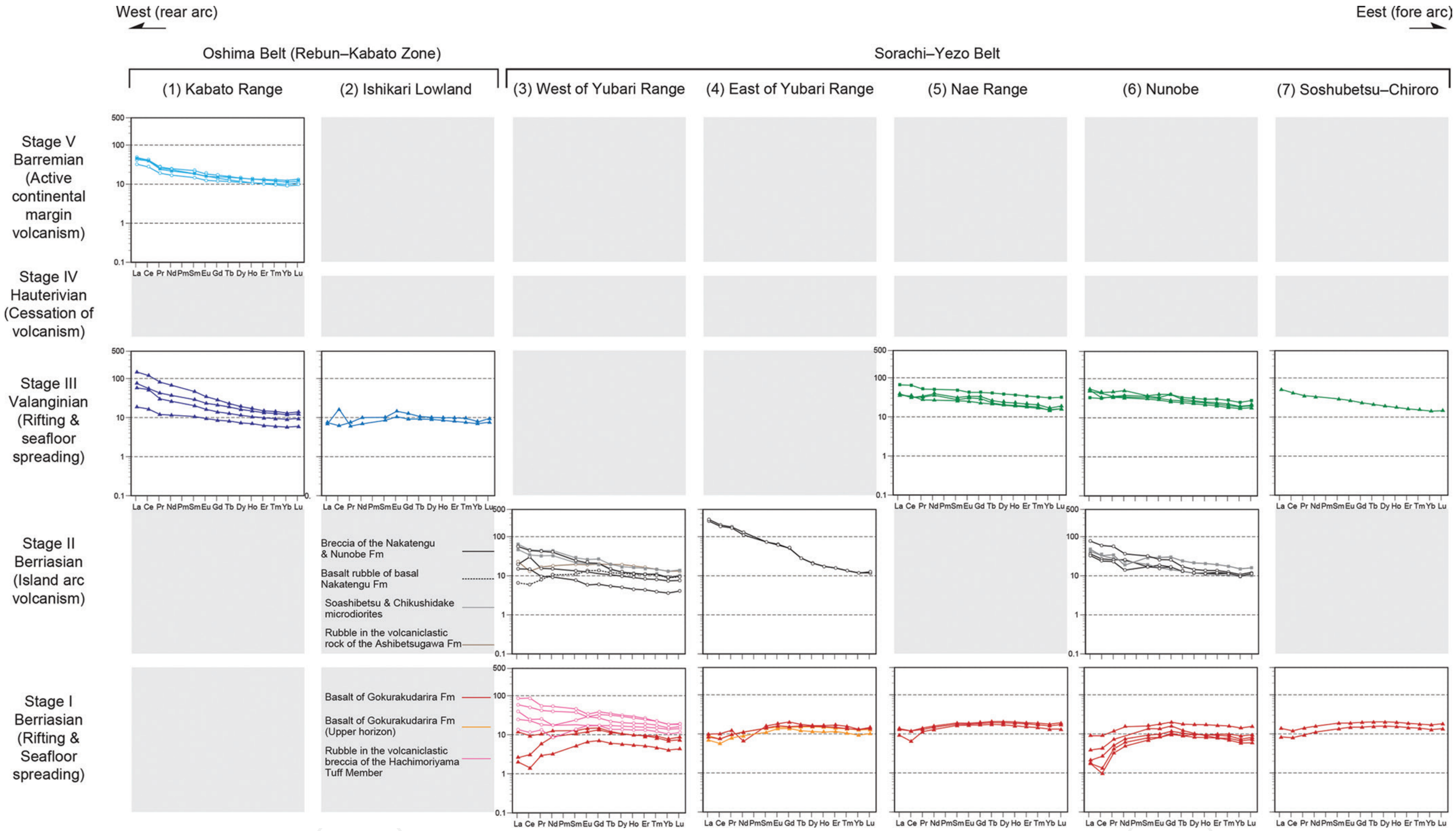

Figure 6. Chondrite-normalized rare earth element patterns for volcanic rocks from the Sorachi and Kumaneshiri groups in the studied sections. Symbols as in **Figure 4**.

The essential lenses in the volcaniclastic rocks in the Hachimoriyama Tuff Member occur mostly in calc-alkaline andesite (**Figures 4** and **8**). The N-MORB-normalized incompatible trace element abundance patterns are characterized by the enrichment of large-ion lithophile elements (LILEs) and depletion of high-field strength elements (HFSEs), with negative anomalies in Ta and Nb abundances relative to N-MORB (**Figure 5**). Chondrite-normalized REE abundance patterns show higher LREE content compared to the content of HREEs (**Figure 6**).

5.2. Rocks of Stage II (Berriasian)

Basalt rubble and gravels from the volcaniclastic rocks in the Ashibetsugawa Formation and basaltic conglomerate of the basal Nakatengu Formation are tholeiitic basalt, showing flat patterns in N-MORB-normalized incompatible trace elements and chondrite-normalized REE patterns resembling those of the basaltic rocks of the underlying Gokurakudaira Formation (**Figures 5** and **6**).

The rubble of volcaniclastic breccia and volcanogenic conglomerate of the Nakatengu and Nunobe formations, as well as the rocks of the Soashibetsu and Chikushidake microdiorites in the areas to the west of the Yubari Range and Nunobe, is plotted in the fields of calc-alkaline andesite (**Figures 4** and **8**). Conversely, the rubble of volcanogenic breccia of the Nakatengu Formation to the east of the Yubari Range is alkali basalt (**Figure 5**). The calc-alkaline andesites and alkali basalts are characterized as being rich in LILEs relative to HFSEs having Ta and Nb trough in the N-MORB-normalized incompatible trace element pattern (**Figure 6**). For the chondrite-normalized REE pattern, LREEs are considerably higher than HREEs. In particular, the alkali basalts of the Nakatengu Formation to the east of the Yubari Range exhibit high LREE/HREE ratios.

5.3. Rocks of Stage III (Late Berriacian-Late Valanginian)

Volcanic and intrusive rocks of the Ogurose Formation of the Sorachi Group and Kumaneshiriyama Formation of the Kumaneshiri Group are mostly occurred in fields of

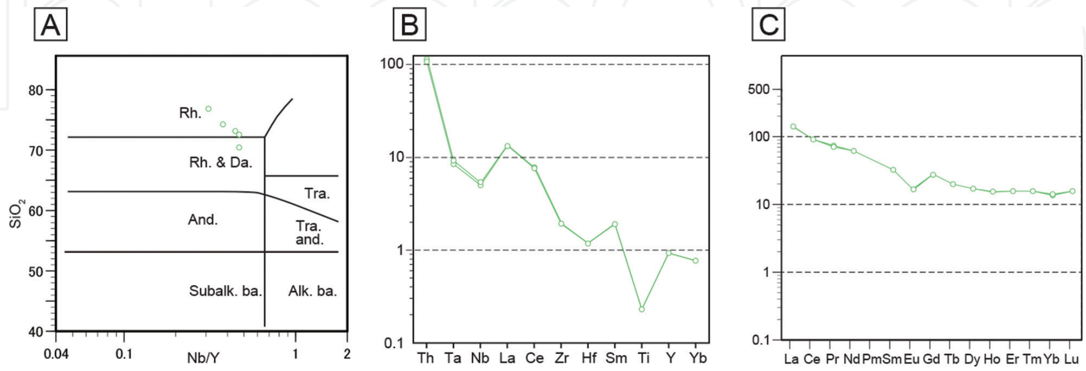

Figure 7. SiO_2 versus Nb/Y diagram (A) and N-MORB-normalized incompatible trace element (B), and chondrite-normalized rare earth element (C) patterns from the Yezo Group. Symbols as in **Figure 4**.

calc-alkaline basalt to andesite, while rocks of the Kumaneshiriyama Formation from the Eniwa borehole are classified as tholeiite basalt (**Figures 4** and **8**).

In the diagram of the N-MORB-normalized incompatible trace element abundances of this stage (**Figure 5**), the igneous rocks of the Sorachi Group and Kumaneshiriyama Formation in the Kabato Range exhibit a high concentration of LILEs relative to that of HFSEs, with a negative anomaly in Ta and Nb contents. **Figure 5** shows that the high LILE/HFSE ratio and depletion in Ta and Nb are prominent in the Kabato Range area, while the tholeiitic basalts of the Kumaneshiriyama Formation at the Eniwa borehole exhibit a flat pattern and are generally depleted in abundance (**Figure 5**). In the chondrite-normalized REE abundance diagram (**Figure 6**), the tholeiite basalts at the Eniwa borehole are the most depleted in this stage and exhibit a flat pattern, while the igneous rocks from other areas are more enriched in abundance and have slightly higher LREE/HREE ratios.

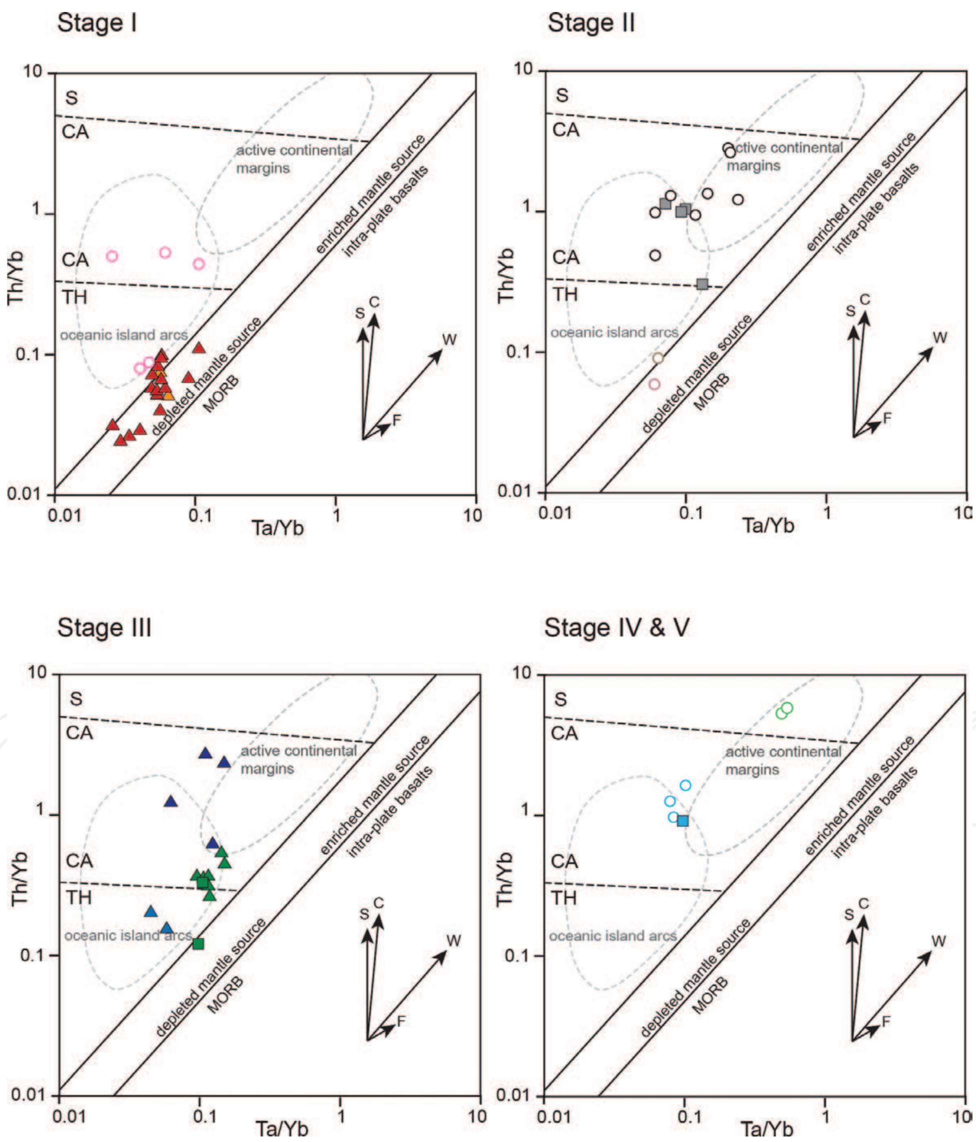

Figure 8. Plot of Th/Yb versus Ta/Yb for igneous rocks from the Sorachi, Kumaneshiri, and Yezo groups. Fields and arrows in the diagram are from Refs. [23, 38]. Symbols as in **Figure 4**.

http://dx.doi.org/10.5772/intechopen.68289

5.4. Rocks of Stage V (Barremian)

The lava and volcanic breccia of the Urausuyama Formation in Kabato Range occur in fields of calc-alkaline basalt to andesite. The diagram of the N-MORB-normalized incompatible trace element patterns shows high LILE and low HFSE contents with marked depletion of Ta and Nb (**Figure 5**). The chondrite-normalized REE patterns show a high concentration of LREEs relative to that of HREEs (**Figure 6**). In the Ta/Tb-Tb/Yb diagram, rocks of this stage occur in the field between the oceanic island arc and active continental margin settings (**Figure 8**).

5.5. Rocks of Stage VI (Aptian-Campanian)

The rhyolite fragments from the Maruyama Formation of the Yezo Group have high LILE/HFSE and LREE/HREE ratios in N-MORB-normalized incompatible trace element and chondrite-normalized REE patterns (**Figure 7**). These rhyolites occur in the active continental margin setting in the Ta/Tb-Tb/Yb diagram (**Figure 8**).

6. Discussion

In this section, we discuss the tectonic models of western-central Hokkaido based on the stratigraphic and petrologic characteristics of the Sorachi and Kumaneshiri groups.

6.1. Stage I (Late Jurassic)

This stage was characterized by extensive eruption of N-MORB-like tholeiitic basalt represented by the Gokurakudaira Formation. The origin of these basaltic rocks is controversial, and several tectonic models have been proposed. Most of the models attributed the origin of these basalts to the mid-ocean ridge, back-arc basin, or oceanic plateau [4, 9, 16, 19, 28, 31].

Although most of the basaltic rocks of the Gokurakudaira Formation have similar geochemical characteristics to those of the N-MORB and back-arc basin, the petrological characteristics of the picrite on the western side of the Yubari Range show extremely high-temperature magmatism, similar to that of Archean komatiite [4]. On the other hand, the basaltic rocks of the Gokurakudaira Formation intercalate the Hachimoriyama Tuff Member, which contains andesitic to dacitic volcaniclastic rocks. The essential andesite lenses show typical supra-subduction zone affinity, with negative anomalies in both Ta and Nb in N-MORB-normalized incompatible trace element patterns (**Figure 5**). These findings suggest that the basaltic rocks of the Gokurakudaira Formation erupted near the island arc. Furthermore, terrigenous sandstone and mudstone also co-occur in this formation, suggesting that extensive eruption of MORB-like basalt and komatiite-like picrite occurred near the continental crust and/or island arc setting.

In order to explain such constraints, the three models shown in **Figure 9** are considered. The first model proposes that the Gokurakudaira Formation was formed by seafloor spreading with slab roll back and asthenospheric upwelling [31]. Takashima et al. [31] considered that

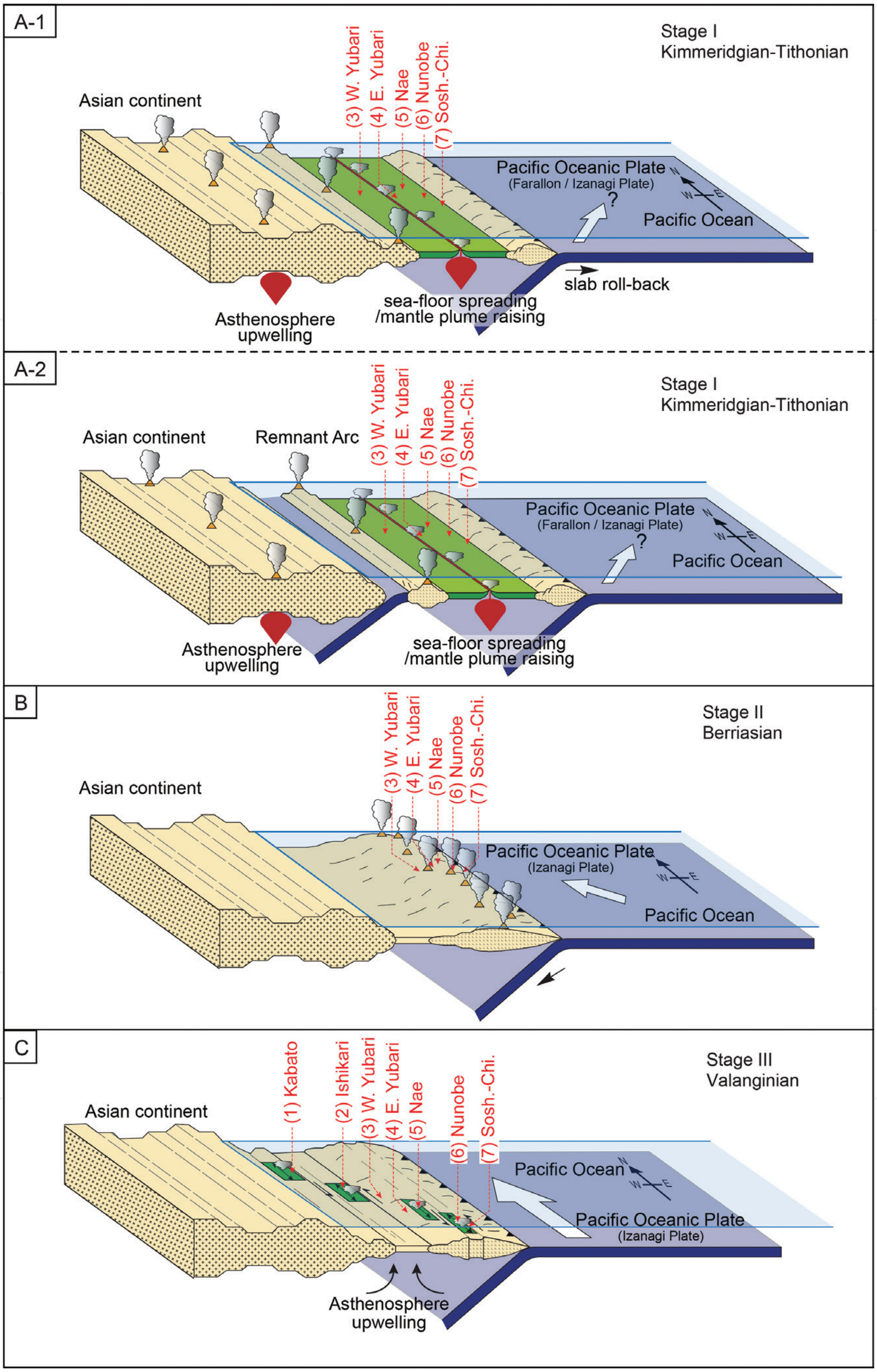

Figure 9. Tectonic models of Late Jurassic-Early Cretaceous Hokkaido. A-1 and A-2 are two plausible models of Stage I (Late Jurassic). B and C are tectonic models of Stage II (Berriasian) and Stage III (Valanginian).

this asthenospheric upwelling could be attributed to the Late Yanshianian Event. In southeast China, back-arc extension and injection of anomalously high-temperature (>1200°C) melts into the lower crust are considered to have occurred during the Late Jurassic [6]. As shown in **Figure 9A-2**, another model of the accretion of oceanic remnant-arc–back-arc basin can also be explainable (**Figure 9A-2**), although no collision zone or remnant arc has been found to date.

On the other hand, the oceanic plateau is also considered to be a strong candidate for the origin of the basaltic rocks of the Gokurakudaira Formation [4, 9, 16]. Large igneous province formation and interactions between depleted mantle and continental crust could also explain the coexistence of basalts of the Gokurakudaira Formation, as well as the andesitic volcaniclastic rocks of the Hachimoriyama Tuff Member and terrigenous sediments of the Shinpaizawa Sandstone Member (**Figure 9A-1**, **A-2**). In the case of the Kerguelen Plateau during the Cretaceous, some basaltic rocks have geochemical signatures that are consistent with a minor contribution from continental crustal material [2, 18]. These rocks also exhibit a prominent trough of Nb and Ta in primitive-mantle-normalized incompatible element abundance patterns, in common with the andesitic rocks of the Hachimoriyama Tuff Member.

6.2. Stage 2 (Berriasian)

The Berriasian Stage is characterized by the formation of andesitic to alkali basaltic volcanoes on the western and eastern sides of the Yubari Range and Nunobe areas. These volcanoes were partly emerged above the sea surface because gravels of oolitic limestones as well as oolitic turbidite beds, which are typically formed in shallow warm intertidal environments, are contained in the volcaniclastic sediments [31].

The volcanoes were formed on the supra-subduction zone because the andesite and microdiorites of this stage show typical island arc characteristics in spider diagrams of N-MORB-normalized incompatible element patterns (**Figure 5**). In the diagram showing Th/Yb-Ta/Yb ratios (**Figure 8**), igneous rocks of this stage were influenced by fluids in the subducting slab and clearly occur in the field of oceanic island arc areas.

Numerous intrusive bodies of microdiorite and diorite occur in the serpentinite bodies of the Horokanai Ophiolite throughout the axial zone of Hokkaido [5]. Although there is no age constraint for these intrusive rocks, N–S trending of microdiorite bodies might indicate that N–S-trending chains of andesitic volcanic edifices were formed in the Sorachi–Yezo Belt during this period (**Figure 9B**).

6.3. Stage III (Late Berriacian–Late Valanginian)

In the Sorachi-Yezo Belt, the emerged andesitic volcanoes subsided into deep marine environments and basaltic-to-basaltic andesitic pillow lava erupted in the areas of the Nae Range, Nunobe, and Soshubetsu–Chiroro. Contemporaneously, submarine eruption of basalt and andesite occurred in the Rebun–Kabato Zone which is predominated by the Kumaneshiriyama Formation.

Basalts and basaltic andesites in the Sorachi–Yezo Belt show typical island arc affinity in N-MORB-normalized incompatible trace element abundance patterns, which exhibit LILE enrichment relative to HFSEs and Nb- and Ta-negative anomalies (**Figure 5**). However, the influence of subduction components is less apparent than those of the previous Stage 2 rocks, as shown in **Figure 8**. The N-MORB-normalized incompatible trace element and chondrite-normalized REE patterns of this stage show that basalts of the Ishikari Lowland are most depleted in both diagrams (**Figures 5** and **6**). Takashima et al. [31] proposed that the formation of pull-apart basins accompanied by seafloor spreading occurred in the Sorachi-Yezo Belt. In conjunction with the present geochemical results, their findings show that asthenospheric upwelling and crustal thinning were most prominent in the Ishikari Lowland, and that the effect of island arc and/or continental crust material increased toward the east and west (**Figure 9C**).

Contemporaneous basaltic-to-rhyolitic volcanism has been recorded along the eastern margin of the Tohoku region (e.g., Yamadori and Harachiyama Formations), suggesting that widespread asthenospheric upwelling occurred along the eastern margin of the continent during this period. Paleomagnetic studies of the Sorachi Group have shown that rocks of Stages I–III were located several thousands of kilometers south of the present position [10].

6.4. Stage IV (Late Valanginian–Hauterivian)

In this period, in situ volcanic activity decreased in both the Rebun–Kabato Zone and the Sorachi–Yezo Belt. Takashima et al. [31] considered that the cessation of volcanism during this period was caused by strike slip movement in the subduction zone.

6.5. Stage V (Late Hauterivian–Barremian)

This stage is characterized by the reappearance of volcanism in the Rebun–Kabato Zone. Although there is no evidence of in situ volcanism in the Sorachi–Yezo Belt, the volcaniclastic turbidities occur frequently on the eastern and western sides of the Yubari Range (**Figure 3**). In the diagram of Th/Yb-Ta/Yb ratios (**Figure 8**), the volcanic rocks of this stage are characterized as being transitional between the oceanic island arc and active continental margins.

6.6. Stage VI (Aptian–Campanian)

The Yezo Group, a fore-arc basin sequence consisting of terrigenous turbidite sandstone and hemipelagic mudstones, started to accumulate in the Sorachi–Yezo Belt in this stage. Abundant felsic tuff beds are also intercalated in the Yezo Group, and the rhyolitic and granitic rocks that formed during this period exhibit a typical continental arc setting (**Figure 8**). In this stage, numerous granitic batholiths were formed in the Oshima Belt as well as along the eastern margin of the Tohoku region.

Acknowledgements

We sincerely thank Jun-ichi Kimura and Yoshitaka Nagahashi for support with the X-ray fluorescence analyses at the Fukushima University, and to Japan Petroleum Exploration Co., Ltd.

for providing samples of the Eniwa SK-1 borehole core. This work was supported by JSPS KAKENHI (Grant Nos. JP24244082 and JP25287130).

Author details

Reishi Takashima[1]*, Hiroshi Nishi[1] and Takeyoshi Yoshida[1,2]

*Address all correspondence to: rtaka@m.tohoku.ac.jp

1 The Center for Academic Resources and Archives, Tohoku University Museum, Tohoku University, Sendai, Japan

2 Institute of Earth Sciences, Graduate School of Science, Tohoku University, Sendai, Japan

References

[1] Du Vivier ADC, Selby D, Condon DJ, Takashima R, Nishi H. Pacific 187Os/188Os isotope chemistry and U–Pb geochronology: Synchroneity of global Os isotope change across OAE 2. Earth Planetary Science Letters. 2015;**428**:204–216

[2] Frey FA, Weis D, Borisova AY, Xu G. Involvement of continental crust in the formation of the Cretaceous Kerguelen Plateau: New perspectives from ODP Leg 120 sites. Journal of Petrology. 2002;**43**:1207–1239

[3] Hasegawa T. Cenomanian–Turonian carbon isotope events recorded in terrestrial organic matter from northern Japan. Palaeogeography, Palaeoclimatology, Palaeoecology. 1997;**130**:251–273.

[4] Ichiyama Y, Ishiwatari A, Kimura J, Senda R, Kawabata H, Tatsumi Y. Picrites in central Hokaido: Evidence of extremely high temperature magmatism in the Late Jurassic ocean recorded in an accreted oceanic plateau. Geology. 2012;**40**:411–414

[5] Igi S, Tanaka K, Hara M, Sato H. Geology of the Horokanai District, with Geological Sheet Map at 1:50,000. Kawasaki: Geological Survey of Japan. 1958: 55 p.

[6] Jiang Y-H, Ling H-F, Jiang S-Y, Fan H-H, Shen W-Z, Ni P. Petrogenesis of a Late Jurassic peraluminous volcanic complex and its high-Mg, potassic, quenched enclaves at Xiangshan, southeast China. Journal of Petrology. 2005;**46**:1121–1154

[7] Jones CE, Jenkyns HC. Seawater strontium isotopes, oceanic anoxic events and seafloor hydrothermal activity in the Jurassic and Cretaceous. American Journal of Science. 2001;**301**:112–149

[8] Kawabe F. Cretaceous stratigraphy in the Oyubari area, central Hokkaido, Japan. Bulletin of the National Science Museum. 2000;**26**(Series C, Geology):9–56

[9] Kimura G, Sakakibara M, Okamura M. Plumes in central Panthalassa? Deductions from accreted oceanic fragments in Japan. Tectonics. 1994;**13**:905–916

[10] Kitagawa Y, Takashima R, Itoh Y. Paleomagnetism of the Sorachi and Yezo Group in the Ashibetsu area, central Hokkaido, Japan. Bulletin of Tohoku University Museum. 2016;(15):109–125

[11] Kiyokawa S. Geology of the Idonnappu Belt, central Hokkaido, Japan: Evolution of a Cretaceous accretionary complex. Tectonics. 1992;**11**:1180–1206

[12] Kondo H. Stratigraphy and geological structure of the Kumaneshiri Group in the Kabato Mountains, Hokkaido, Japan. Journal of Geological Society of Japan. 1991;**97**:357–376

[13] Labails C, Olivet J-L, Aslanian D, Roest WR. An alternative early opening scenario for the Central Atlantic Ocean. Earth and Planetary Science Letters. 2010;**297**:355–368

[14] Li X-H, Chung S-L, Zhou H, Lo C-H, Liu Y, Chen C-H. Jurassic intraplate magmatism in southern Hunan-eastern Guangxi: 40Ar/39Ar dating, geochemistry, Sr-Nd isotopes and implications for the tectonic evolution of SE China. In: Malpas J, Fletcher CJN, Ali JR, Aitchison JC, editors. Aspect of the Tectonic Evolution of China. Geological Society. Vol. 226. London: Special Publications; 2004. pp. 193–215

[15] McArthur JM, Howarth RJ, Bailey TR. Strontium isotope stratigraphy: LOWESS version 3: Best fit to the marine Sr-isotope curve for 0–509 Ma and accompanying look-up table for deriving numerical age. The Journal of Geology. 2001;**109**:155–170

[16] Nagahashi T, Miyashita S. Petrology of the greenstones of the lower Sorachi Group in the Sorachi-Yezo belt, central Hokkaido, Japan, with special reference to discrimination between oceanic plateau basalts and mid-oceanic ridge basalts. The Island Arc. 2002;**11**:122–141

[17] Nagata M, Kito N, Niida K. The Kumaneshiri Group in the Kabato Mountains: The age and nature as an Early Cretaceous volcanic arc. In: Editorial Committee of Geology and Tectonics of Hokkaido, editors. Geology and Tectonics of Hokkaido. Sapporo: Monograph of the Association for the Geological Collaboration in Japan. Vol. 31. 1986. pp. 379–402

[18] Neal CR, Mahoney JJ, Chazey WJ. Mantle sources and the highly variable role of continental lithosphere in basalt petrogenesis of the Kerguelen Plateau and Broken Ridge LIP: Results from ODP Leg 183. Journal of Petrology. 2002;**43**:1177–1205

[19] Niida K, Kito N. Cretaceous arc–trench systems in Hokkaido. In: Editorial Committee of Geology and Tectonics of Hokkaido, editors. Geology and Tectonics of Hokkaido. Sapporo: Monograph of the Association for the Geological Collaboration in Japan. Vol. 31. 1986. pp. 379-402.

[20] Nishi H, Takashima R, Hatsugai T, Saito T, Moriya K, Ennyu A, Sakai T. Planktonic foraminiferal zonation in the Cretaceous Yezo Group, Central Hokkaido, Japan. Journal of Asian Earth Sciences. 2003;**21**:867–886

[21] Okada H. Migration of ancient arc-trench systems. In: Dott RJH, Shaver RH, editors. Modern and Ancient Geosynclinals Sedimentation. Society of Economic Paleontologists and Mineralogists, Special Publication No. 19; 1974. pp. 311–320

[22] Oxman VS. Tectonic evolution of the Mesozoic Verkhoyansk-Kolyma belt (NE Asia). Tectonophysics. 2003;**365**:45–76

[23] Pearce JA. Trace element characteristics of lavas from destructive plate boundaries. In: Thorpe ES, editors. Andesites. New York, NY: John Wiley and Sons; 1982. pp. 525–548

[24] Quidelleur X, Paquette JL, Fiet N, Takashima R, Tiepolo M, Desmares D, Nishi H, Grosheny D. New U-Pb (ID-TIMS and LA-ICPMS) and 40Ar/39Ar geochronological constraints of the Cretaceous geologic time scale calibration from Hokkaido (Japan). Chemical Geology. 2011;**286**:72–83

[25] Sun S-S, McDounough WF. Chemical and isotopic systematics of oceanic basalts: implications for mantle composition and processes. In: Saunders AD, Norry MJ, editors. Magmatism in the Ocean Basins. Geological Society, London, Special Publications. Vol. 42; 1989. pp. 313–345

[26] Suzuki N, Kurita H, Takashima R. Earliest Cretaceous radiolarian assemblages from a deep borehole section in the southern Ishikari Plain, central Hokkaido, and their implications. In: The 106th Annual Meeting of the Geological Society of Japan; October 9-10; Nagoya. Tokyo: The Geological Society of Japan; 1999. p. 307.

[27] Taira A. Tectonic evolution of the Japanese island arc system. Annual Review of Earth and Planetary Sciences. 2001;**29**:109–134

[28] Takashima R, Nishi H, Yoshida T. Geology, petrology and tectonic setting of the Late Jurassic ophiolite in Hokkaido, Japan. Journal of Asian Earth Sciences. 2002;**21**:197–215

[29] Takashima R, Nishi H, Miyamoto Y, Yoshida T. Geology and stratigraphy of the Sorachi and Yezo groups in the Tokyo University Forests in Hokkaido, Japan. Bulletin of Tokyo University Forests. 2002;**108**:57–76

[30] Takashima R, Kawabe F, Nishi H, Moriya K, Wani R, Ando H. Geology and stratigraphy of forearc basin sediments in Hokkaido, Japan: Cretaceous environmental events on the north-west Pacific margin. Cretaceous Research. 2004;**25**:365–390

[31] Takashima R, Nishi H, Yoshida T. Late Jurassic–Early Cretaceous intra-arc sedimentation and volcanism linked to plate motion change in northern Japan. Geological Magazine. 2006;**143**:753–770

[32] Takashima R, Nishi H, Yamanaka T, Hayashi K, Waseda A, Obuse A, Tomosugi T, Deguchi N, Mochizuki S. High-resolution terrestrial carbon isotope and planktonic foraminiferal records of the Upper Cenomanian to the Lower Campanian in the Northwest Pacific. Earth and Planetary Science Letters. 2010;**289**:570–582

[33] Takashima R, Nishi H, Yamanaka T, Tomosugi T, Fernando AG, Tanabe K, Moriya K, Kawabe F, Hayashi K. Prevailing toxic environments in the Pacific Ocean during the mid-Cretaceous Oceanic Anoxic Event 2. Nature Communications. 2011;**2-234.** DOI: 10.1038/ncomms1233

[34] Taketani, Y. Cretaceous radiolarian biostratigraphy of the Urakawa and Obira areas, Hokkaido. Science Reports of the Tohoku University. Second Series, Geology. 1982;**52**: 1–75

[35] Ueda H, Miyashita S. Tectonic accretion of a subducted intraoceanic remnant arc in Cretaceous Hokkaido, Japan, and implications for evolution of the Pacific northwest. The Island Arc. 2005;**14**:582–598

[36] Van der Voo R, Spakman W, Bijwaard H. Mesozoic subducted slabs under Siberia. Nature. 1999;**397**:246–249

[37] Vissers RLM, van Hinsbergen DJJ, Meijer PT, Piccardo GB. Kinematics of Jurassic ultra-slow spreading in the Piemonte Ligurian ocean. Earth and Planetary Science Letters. 2013;**380**:138–150.

[38] Wilson M. Igneous Petrogenesis. London: Chapman & Hall; 1989. p. 466.

[39] Winchester JA, Floyd PA. Geochemical discrimination of different magma series and their differentiation products using immobile elements. Chemical Geology. 1977;**20**: 324–343

[40] Zhou XM, Li WX. Origin of Late Mesozoic igneous rocks in Southeastern China: Implications for lithosphere subduction and underplating of mafic magmas. Tectonophysics. 2000; **326**:269–287

[41] Zonenshain LP, Kuzmin MI, Natapovm LM. Geology of the USSR: A Plate-Tectonic Synthesis. Washington, DC: AGU; 1990. p. 242.